

## Research Article

# Integration of High-Performance Nanocrystalline TiO<sub>2</sub> Photoelectrodes for N719-Sensitized Solar Cells

Ke-Jian Jiang,<sup>1</sup> Jin-Ming Zhou,<sup>1</sup> Kazuhiro Manseki,<sup>2</sup> Qi-Sheng Liu,<sup>1</sup> Jin-Hua Huang,<sup>1</sup> Yan-lin Song,<sup>1</sup> and Shozo Yanagida<sup>3</sup>

<sup>1</sup> Laboratory of New Materials, Institute of Chemistry, Chinese Academy of Sciences, Beijing 100190, China

<sup>2</sup> Graduate School of Engineering, Environmental and Renewable Energy System (ERES) Division, Gifu University, 1-1, Yanagida, Gifu 501-1193, Japan

<sup>3</sup> ISIR, Osaka University, 2-1, Mihoga-oka, Ibaraki, Osaka 567-0047, Japan

Correspondence should be addressed to Shozo Yanagida; yanagida@mls.eng.osaka-u.ac.jp

Received 12 February 2013; Accepted 21 April 2013

Academic Editor: Theodoros Dimopoulos

Copyright © 2013 Ke-Jian Jiang et al. This is an open access article distributed under the Creative Commons Attribution License, which permits unrestricted use, distribution, and reproduction in any medium, provided the original work is properly cited.

We report on enhanced performance of N719-sensitized TiO<sub>2</sub> solar cells (DSCs) incorporating size and photoelectron diffusion-controlled TiO<sub>2</sub> as sensitizer-matched light-scatter layers on conventional nanocrystalline TiO<sub>2</sub> electrodes. The double-layered N719/TiO<sub>2</sub> composite electrode with a high dye-loading capacity exhibits the diffused reflectance of more than 50% in the range of  $\lambda = 650\text{--}800$  nm, even when the films are coupled with the titania nanocrystalline underlayer in the device. As a result, the increased near-infrared light-harvesting produces a high light-to-electricity conversion efficiency of over 9% mainly due to the significant increase of  $J_{sc}$ . Such an optical effect of the NIR-light scattering TiO<sub>2</sub> electrodes will be beneficial when the sensitizers with low molar extinction coefficients, such as N719, are introduced in the device.

## 1. Introduction

Dye-sensitized solar cells (DSCs) have been explored from both academic and industry world as a promising alternative to the conventional silicon-based photovoltaic devices [1–3], and efficiencies of over 12% have been achieved [4]. In this cell, a wide band-gap nanostructured semiconductor electrode (typically, TiO<sub>2</sub>) is employed to support a large surface area, on which dye molecules are assembled to improve the light harvesting of the dyed electrode. A great deal of effort has been focused on the development of effective panchromatic sensitizers or cosensitizers for efficient solar light harvesting in DSC devices. On the other hand, the light-harvesting efficiency of DSC can be promoted by introducing a sophisticated structure in the photoelectrode, in which the photon path length is increased by the confinement of incident solar energy light. Usami made the theoretical finding that lightscattering in DSCs will be optimized if the diameter of TiO<sub>2</sub> nanocrystals is twice the size of the wavelength of incident light [5]. The effect has been verified in the DSCs, in which a TiO<sub>2</sub> layer built from

submicrometer-sized TiO<sub>2</sub> particles was employed in combination with a transparent nanostructured TiO<sub>2</sub> layer [6–8]. In addition, TiO<sub>2</sub> (or ZnO) photoelectrodes with submicrometer-sized beads, hollow spheres, and tubes have been widely investigated [9–15].

As an alternative to such a large particle light-scattering material, TiO<sub>2</sub> layers with periodic pore structures exhibiting photonic band gaps have been applied for DSCs to enhance light harvesting efficiency [16–21]. Such light scattering TiO<sub>2</sub> layers, however, required an elaborate multistep synthesis. On the other hand, Hore et al. reported scattering of light on disordered spherical voids in TiO<sub>2</sub> electrodes for enhanced DSC performance. The DSC with 400 nm void layers gave a higher efficiency (6.7%) as compared to the cavity-free layer (5.4%) [22]. While the overall efficiency was improved, a slight increase of  $J_{sc}$  was observed and the appreciable increase of fill factors resulted in the 18% increment of conversion efficiency. Despite a number of nanostructured TiO<sub>2</sub> photoelectrodes reported as mentioned previously, the cell performance originated from spherical void-centered TiO<sub>2</sub> has still been poorly understood. Most importantly,

little has been reported on an enhancement of near-infrared-(NIR-) light response in IPCE [22, 23]. As organic dye molecules with large extinction coefficients even in the red region were used, the results represent a compromise between slight light scattering and enhanced mobility of viscous electrolytes in the large hollow cavities [23]. In this paper we demonstrate optimized effects of scattering on submicron  $\text{TiO}_2$  particles with spherical cavities on quantum efficiencies of light-to-electricity conversion of N719-sensitized solar cells at a NIR region, where the N719 dye has a low extinction coefficient. Accordingly, we prepared a  $\text{TiO}_2$  layer containing 600 nm large spherical cavities and combined successively with the conventional nanocrystalline  $\text{TiO}_2$  layer. We then applied the hollow-cavity-based  $\text{TiO}_2$ /nanocrystalline  $\text{TiO}_2$  double composite electrodes to N719-sensitized DSC. The DSC exhibited a maximum conversion efficiency of 9.25% versus 6.38% for the reference cell with single conventional  $\text{TiO}_2$  electrodes. We demonstrated that the hollow-cavity-based  $\text{TiO}_2$  contributes not only to the enhanced absorption of near-infrared photons but also to effective dye sensitization as evidenced by the remarkable enhancement of  $J_{sc}$  in the performance. It should be noted that the effective electron diffusion coefficient of the dye-coated light-scattering  $\text{TiO}_2$  layer also plays a crucial role in the improved DSC performance.

## 2. Materials and Methods

Polyethyleneglycol (PEG,  $M_w = 20,000$ ) was purchased from Fluka Co. The Ru dye, N719 (cis-bis(isothiocyanato) bis(2,2'-bipyridyl-4,4'-dicarboxylato)-ruthenium (II) bis-tetrabutylammonium) was purchased from Solaronix S.A. Iodine, 1-propyl-3-methylimidazolium iodide, valeronitrile, lithium iodide, and *tert*-butylpyridine were purchased from Aldrich without purification.

**2.1. Preparation of DSCs.** A 60 nm dense  $\text{TiO}_2$  layer was deposited on a patterned ITO-coated glass substrates ( $10 \Omega/\square$ , Nippon Sheet Glass) by spin coating technique with tetraisopropyl orthotitanate in ethanol, as reported previously [24]. The  $\text{TiO}_2$  films, served as a blocking layer in DSCs, were annealed in air at  $500^\circ\text{C}$  for 30 minutes. Following this, a  $\text{TiO}_2$  paste with 20 nm particle size was deposited by doctor blade technique on the blocking layer, where the  $\text{TiO}_2$  paste was prepared according to the previous report [25]. A transparent  $\text{TiO}_2$  underlayer was achieved after the calcination at  $500^\circ\text{C}$  for 30 minutes. Functional polystyrene spheres (PS) (560 nm in size) were synthesized according to our previous method [26]. The resulting latex spheres were used directly without purification. The polystyrene spheres (PS) were fabricated via batch emulsion polymerization, where styrene was mixed with methyl methacrylate (MMA) and acrylic acid (AA). For the preparation of the spherical cavity-based light-scattering  $\text{TiO}_2$  layer, as prepared spheres were dispersed in the  $\text{TiO}_2$  colloid with the particle size of about 20 nm as a coating paste for the preparation of the overlayer. The PS sphere, the previously mentioned  $\text{TiO}_2$  colloid, and PEG were mixed in water with ratio of 1/0.5/0.3 ( $\text{TiO}_2$ /PS/PEG, by weight) and homogenized with a stirring bar and ultrasonication. The

resulting paste was deposited as a light-scattering layer on the underlayer, followed by the same calcination procedure mentioned previously. Finally, the double-layered  $\text{TiO}_2$  film was impregnated with 0.2 M  $\text{TiCl}_4$  aqueous solution at room temperature overnight and then calcinated again at  $500^\circ\text{C}$  for 30 minutes. After cooling to about  $120^\circ\text{C}$ , the films were emerged overnight in 1:1 v/v acetonitrile and *tert*-butyl alcohol solvent mixture containing N719 dye at a concentration of 0.3 mM. A Pt-sputtered FTO glass was used as a counter electrode. The electrolyte was composed of 0.6 M 1-propyl-3-methylimidazolium iodide, 0.1 M LiI, 0.04 M  $\text{I}_2$ , and 0.5 M *tert*-butylpyridine in the mixture of acetonitrile and valeronitrile (1:1, by volume).

**2.2. Characterization and Photoelectric Measurements.** The SEM images of titania films were obtained with a field-emission SEM (JEOL JSM-4800, Japan). The optical reflection measurement was performed using an UV-vis spectrophotometer (U-3010, HITACHI) equipped with an integrating sphere.

The incident photon-to-current conversion efficiency (IPCE) for solar cells was measured by using a commercial setup (PV-25 DYE, JASCO) equipped with a monochromator. A 300 W Xenon lamp was employed as a light source for the generation of a monochromatic beam. Calibrations were performed with a standard silicon photodiode. IPCE is defined by  $\text{IPCE}(\lambda) = hc J_{sc}/e\phi\lambda$ , where  $h$  is Planck's constant,  $c$  is the speed of light in a vacuum,  $e$  is the electronic charge,  $\lambda$  is the wavelength in meters (m),  $J_{sc}$  is the short-circuit photocurrent density ( $\text{A m}^{-2}$ ), and  $\phi$  is the incident radiation flux ( $\text{W m}^{-2}$ ). The photocurrent-voltage ( $I$ - $V$ ) characteristics were recorded using a computer-controlled Keithley 2400 source meter under air mass (AM) 1.5 simulated illumination ( $100 \text{ mw cm}^{-2}$ , Oriel, 67005). The active area of the samples was about  $0.2 \text{ cm}^2$ , controlled by an aperture mask to prevent extra light from coming through the lateral space.  $I$ - $V$  data were well within experimental error.

## 3. Results and Discussion

As shown in Figure 1(a), the latex PS sphere holds a hard PS core with an elastomeric PMMA/PAA shell and presents a monodispersity with the size of about 560 nm (Figure 1(b)). The  $\text{TiO}_2$  overlayer was prepared through a simple mixing of submicrometer-size polystyrene (PS) spheres and nano sized  $\text{TiO}_2$  particles, followed by subsequent coating and calcinations on a transparent  $\text{TiO}_2$  underlayer. The PS spheres vanish during the calcination process.

The SEM image in Figure 2(a) shows a top surface image of the  $\text{TiO}_2$  overlayer. It is very clear that homogeneous spherical voids spread on the whole surface with the size of around 600 nm. Figure 2(b) shows a top surface image of the  $\text{TiO}_2$  transparent layer, which presents a porous structure comprised of 20 nm sized  $\text{TiO}_2$  particles. The cross-sectional image of the corresponding double-layer electrode is shown in Figure 2(c), where the  $8 \mu\text{m}$  thick transparent nanoporous  $\text{TiO}_2$  underlayer and the  $6 \mu\text{m}$  thick  $\text{TiO}_2$  overlayer are formed without cracks.

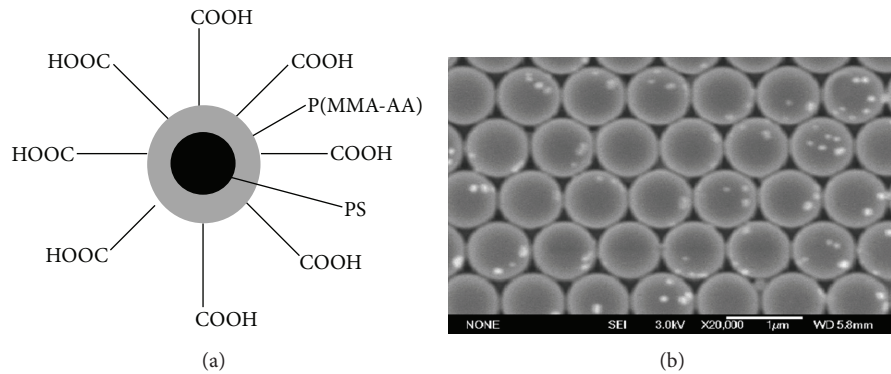


FIGURE 1: (a) A schematic structure of the functionalized polystyrene spheres. (b) A SEM image of the PS spheres with a diameter of 560 nm.

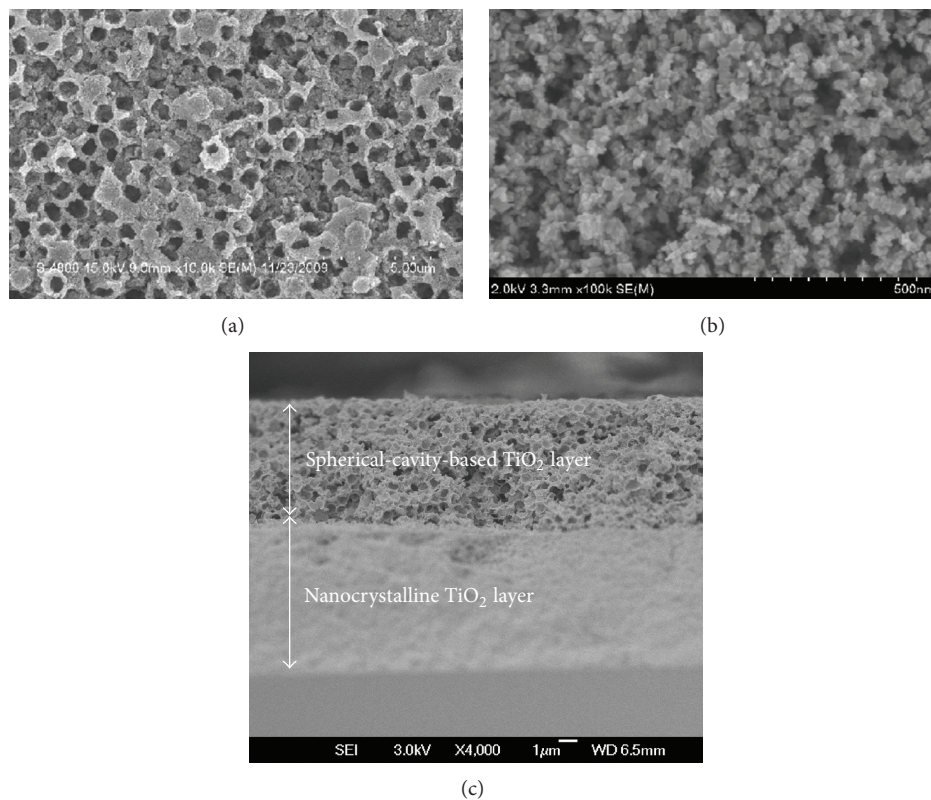


FIGURE 2: Scanning electron micrographs of (a) the top view of a spherical-cavity-based  $\text{TiO}_2$  film, (b) the top view of a nanocrystalline  $\text{TiO}_2$  film, (c) cross-sectional view of the double-layer  $\text{TiO}_2$  film with a nanocrystalline  $\text{TiO}_2$  layer and a spherical-cavity-based  $\text{TiO}_2$  layer.

In order to investigate the light-scattering ability of the overlayer, UV-vis reflectance spectra were recorded for a  $6\ \mu\text{m}$  thick spherical-cavity-based  $\text{TiO}_2$  film with and without sensitization by using a standard N719 dye, and an  $8\ \mu\text{m}$ -thick nanostructured  $\text{TiO}_2$  film was employed for comparison, as shown in Figure 3. For the film without the dye loading, the reflectance of the overlayer is more than 70% in the whole UV-vis region, indicating that more than 90% of the light reflecting efficiency can be achieved by the overlayer when considering the absorption and reflection by the FTO glass substrate. By contrast the reflectance of the transparent nanostructured  $\text{TiO}_2$  underlayer is less than 30%. After the

dye adsorption, the reflectance was significantly decreased in the spectral range by around 535 nm for both the layers, where N719 dye has the maximum absorption, indicating that the reduction is mainly ascribed to the light absorption by the dye. Most importantly, the diffused reflectance of the  $\text{TiO}_2$ /dye composite film is found to be more than 50% in the range of  $\lambda = 650\text{--}800\ \text{nm}$  after the dye loading for the overlayer.

We tested the double composite films as DSC photoelectrodes (denoted as sample 1) consisting of a  $8\ \mu\text{m}$  thick nanostructured  $\text{TiO}_2$  underlayer and a  $6\ \mu\text{m}$  thick overlayer, in which a single-layer  $\text{TiO}_2$  electrode only with the  $8\ \mu\text{m}$

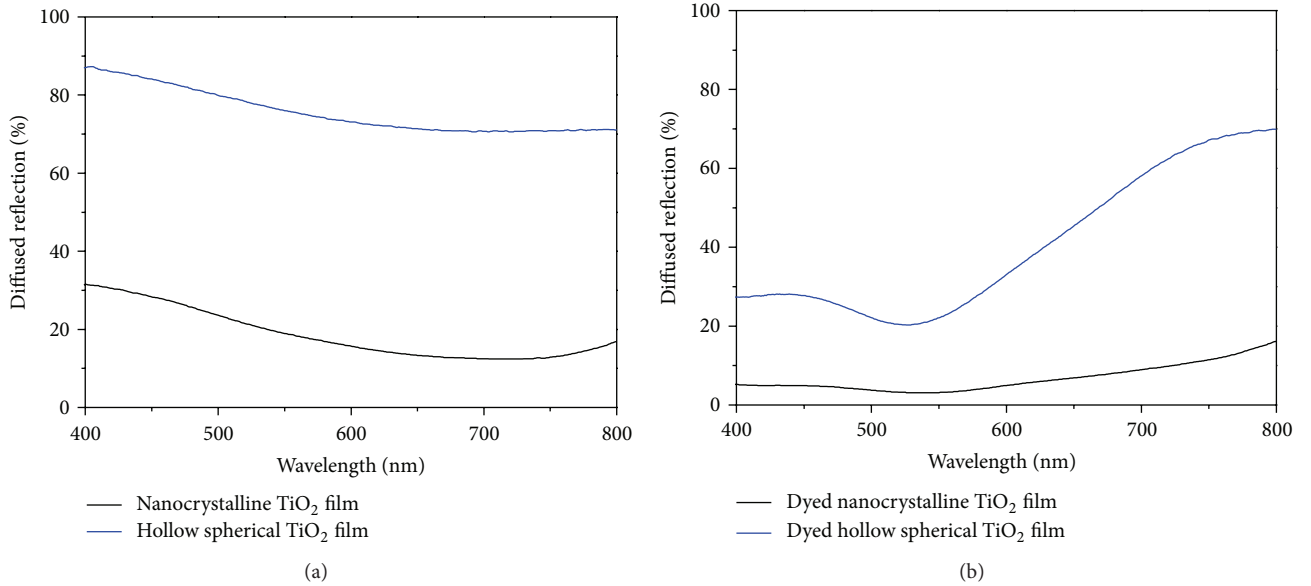


FIGURE 3: Diffused reflectance spectra of a nanocrystalline  $\text{TiO}_2$  film ( $8 \mu\text{m}$  thick) and a spherical-cavity-based  $\text{TiO}_2$  film ( $6 \mu\text{m}$  thick) without (a) and with (b) N719 dye loading.

TABLE 1: Photovoltaic characteristics of samples 1, 2, and 3 measured under AM1.5 illumination ( $100 \text{ mW cm}^{-2}$ ). Each data represents the average of three cells with active area of  $0.2 \text{ cm}^2$ .

Sample	Thickness [ $\mu\text{m}$ ]	$J_{sc}$ [ $\text{mA/cm}^2$ ]	$V_{oc}$ [V]	FF	$\eta$ [%]	Adsorbed dye [ $\mu \text{mol cm}^{-2}$ ]
1	8 + 6	$18.40 \pm 0.05$	$0.73 \pm 0.02$	$0.69 \pm 0.01$	$9.25 \pm 0.05$	1.163
2	8	$13.04 \pm 0.03$	$0.73 \pm 0.02$	$0.67 \pm 0.01$	$6.38 \pm 0.05$	1.012
3	10	$14.86 \pm 0.03$	$0.70 \pm 0.02$	$0.68 \pm 0.01$	$7.07 \pm 0.05$	1.171

thick  $\text{TiO}_2$  underlayer (sample 2) was used for comparison. The current-voltage characteristics are shown in Figure 4 and Table 1. The conversion efficiency ( $\eta$ ) was improved from 6.38% for sample 2 to 9.25% for sample 1, corresponding to the 45% increment. The improved efficiency was mainly caused by the increase of the short-circuit current density ( $J_{sc}$ ) from  $13.04 \text{ mA cm}^{-2}$  to  $18.40 \text{ mA cm}^{-2}$ , while the  $V_{oc}$ s and fill factors are the same or comparable for the two samples. It should be noted that, in the overlayer, the submicro-meter sized voids are surrounded by the nanostructured  $\text{TiO}_2$  film with the  $\text{TiO}_2$  particles of 20 nm. The dye molecules can be absorbed on the overlayer to contribute to the increment of  $J_{sc}$  in the double layer. In order to evaluate the effect of dye absorption in the overlayer on  $J_{sc}$ , the one-layer nanostructured  $\text{TiO}_2$  electrode with a thickness of  $10 \mu\text{m}$  was prepared (sample 3), by considering the amount of the dye loading for fair comparison (the porosity of  $\text{TiO}_2$  overlayer :  $\sim 80\%$ ). The amounts of the absorbed dyes were determined for the three different electrodes by measuring the eluted dye concentration from the  $\text{TiO}_2$  electrodes as shown in Table 1. The dye adsorption capacity was comparable for samples 1 and 3, suggesting that the scattering layer maintains a high dye-adsorption capacity. As shown in Table 1, sample 3 with the  $10 \mu\text{m}$  thick  $\text{TiO}_2$  electrode gave  $14.86 \text{ mA cm}^{-2}$  of  $J_{sc}$ , which was much lower than that of sample 1. A further comparison between sample 2 and sample 3 showed only

a slight increase ( $1.82 \text{ mA cm}^{-2}$ ) in  $J_{sc}$ . On the other hand, the reflectance for sample 1 was significantly higher across the visible part of the spectrum than that of a single-layer  $\text{TiO}_2$  cell as mentioned previously. Therefore, these results indicated that the marked increment in  $J_{sc}$  for sample 1 as compared to 3 is ascribed to the stronger light scattering, particularly at a red to near-infrared light region. It is thus postulated that both the light-scattering property and high dye-loading capacity from the integrated nanocrystalline composite electrodes resulted in the significant increase of IPCE as shown in Figure 5. In addition, it should be noted that the unaffected and effective electron diffusion coefficient in the double-layered  $\text{TiO}_2$  is essential for the improved IPCE in sample 1.

#### 4. Conclusions

We applied a facile colloidal template method for the preparation of spherical-cavity-based  $\text{TiO}_2$ /nanocrystalline  $\text{TiO}_2$  double composite layers as a strong near-infrared light-scattering layer for N719-sensitized solar cells, which is particularly useful for the significant gain of photocurrents. The DSC fabricated by using double-layered electrodes composed of the scattering layer and the nanocrystalline  $\text{TiO}_2$  layer produced a higher conversion efficiency of 9.25% versus 6.38% for the reference cell with a single  $\text{TiO}_2$  electrode

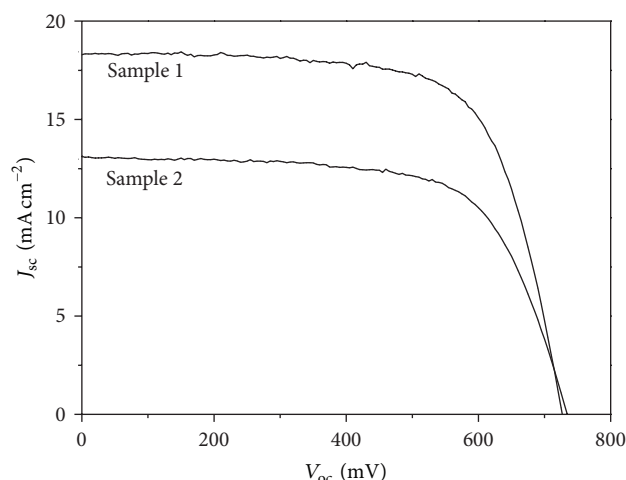


FIGURE 4: Photocurrent and voltage curves for samples 1 and 2. Both measurements were performed under AM 1.5 G with the active area of  $0.2 \text{ cm}^2$ .

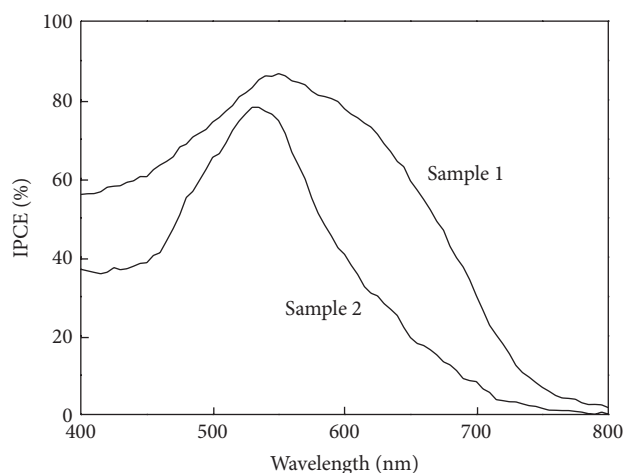


FIGURE 5: Incident monochromatic photon-to-current conversion efficiency (IPCE) as a function of excitation wavelength for samples 1 and 2.

with the comparable thickness. The results obtained from our facile photon capture approach could open up new perspectives of exploiting low-cost and high-efficiency DSCs with a wide range of newly developed dye molecules and electrolytes.

## Conflict of Interests

The authors declare that there is no conflict of interests.

## Acknowledgments

The authors would like to acknowledge the National 863 Program (no. 2011AA050521) and 973 Program (no. 2006CB806200), National Science Foundation of China (nos. 20774103, 50625312, 60601027, 20421101, and U0634004), (No. 50973105), and the Koshiyama Research Grant in Japan for financial support.

## References

- [1] B. O'Regan and M. Grätzel, "A low-cost, high-efficiency solar cell based on dye-sensitized colloidal  $\text{TiO}_2$  films," *Nature*, vol. 353, pp. 737–740, 1991.
- [2] S. Yanagida, Y. You, and K. Manseki, "Iodine/Iodide-Free Dye-Sensitized Solar Cells," *Accounts of Chemical Research*, vol. 42, no. 11, pp. 1827–1838, 2009.
- [3] J. Xia and S. Yanagida, "Strategy to improve the performance of dye-sensitized solar cells: Interface engineering principle," *Solar Energy*, vol. 85, no. 12, pp. 3143–3159, 2011.
- [4] A. Yella, H. W. Lee, H. N. Tsao et al., "Porphyrin-sensitized solar cells with cobalt (II/III)-based redox electrolyte exceed 12 percent efficiency," *Science*, vol. 334, no. 6056, pp. 629–634, 2011.
- [5] A. Usami, "Theoretical simulations of optical confinement in dye-sensitized nanocrystalline solar cells," *Solar Energy Materials and Solar Cells*, vol. 64, no. 1, pp. 73–83, 2000.
- [6] C. J. Barbé, F. Arendse, P. Comte et al., "Nanocrystalline titanium oxide electrodes for photovoltaic applications," *Journal of the American Ceramic Society*, vol. 80, no. 12, pp. 3157–3171, 1997.
- [7] S. Ito, P. Comte, P. Chen et al., "Fabrication of screen-printing pastes from  $\text{TiO}_2$  powders for dye-sensitized solar cells," *Progress in Photovoltaics*, vol. 15, no. 7, pp. 603–612, 2007.
- [8] Y. Chiba, A. Islam, Y. Watanabe, R. Komiya, N. Koide, and L. Han, "Dye-sensitized solar cells with conversion efficiency of 11.1%," *Japanese Journal of Applied Physics*, vol. 45, no. 24-28, pp. L638–L640, 2006.
- [9] T. P. Chou, Q. Zhang, G. E. Fryxell, and G. Cao, "Hierarchically structured ZnO film for dye-sensitized solar cells with enhanced energy conversion efficiency," *Advanced Materials*, vol. 19, no. 18, pp. 2588–2592, 2007.
- [10] D. H. Chen, F. Z. Huang, Y. -B. Cheng, and R. A. Caruso, "Mesoporous anatase  $\text{TiO}_2$  beads with high surface areas and controllable pore sizes: a superior candidate for high-performance dye-sensitized solar cells," *Advanced Materials*, vol. 21, no. 21, pp. 2206–2210, 2009.
- [11] I. G. Yu, Y. J. Kim, H. J. Kim, C. Lee, and W. I. Lee, "Size-dependent light-scattering effects of nanoporous  $\text{TiO}_2$  spheres in dye-sensitized solar cells," *Journal of Materials Chemistry*, vol. 21, no. 2, pp. 532–538, 2011.
- [12] H. J. Koo, Y. J. Kim, Y. H. Lee, W. I. Lee, K. Kim, and N. G. Park, "Nano-embossed Hollow Spherical  $\text{TiO}_2$  as Bifunctional Material for High-Efficiency Dye-Sensitized Solar Cells," *Advanced Materials*, vol. 20, no. 1, pp. 195–199, 2008.
- [13] S. C. Yang, D. J. Yang, J. Kim et al., "Hollow  $\text{TiO}_2$  Hemispheres Obtained by Colloidal Templating for Application in Dye-Sensitized Solar Cells," *Advanced Materials*, vol. 20, no. 5, pp. 1059–1064, 2008.
- [14] D. Li, P. C. Chang, C. J. Chien, and J. G. Lu, "Applications of tunable  $\text{TiO}_2$  nanotubes as nanotemplate and photovoltaic device," *Chemistry of Materials*, vol. 22, no. 20, pp. 5707–5711, 2010.
- [15] J. Yu, J. Fan, and L. Zhan, "Dye-sensitized solar cells based on hollow anatase  $\text{TiO}_2$  spheres prepared by self-transformation method," *Electrochimica Acta*, vol. 55, no. 3, pp. 597–602, 2010.
- [16] S. H. A. Lee, N. M. Abrams, P. G. Hoertz, G. D. Barber, L. I. Halaoui, and T. E. Mallouk, "Coupling of titania inverse opals to nanocrystalline titania layers in dye-sensitized solar cells," *Journal of Physical Chemistry B*, vol. 112, no. 46, pp. 14415–14421, 2008.
- [17] A. Mihi, M. E. Calvo, J. A. Anta, and H. Miguez, "Spectral response of opal-based dye-sensitized solar cells," *Journal of Physical Chemistry C*, vol. 112, pp. 13–17, 2008.

- [18] S. Nishimura, N. Abrams, B. A. Lewis et al., "Standing wave enhancement of red absorbance and photocurrent in dye-sensitized titanium dioxide photoelectrodes coupled to photonic crystals," *Journal of the American Chemical Society*, vol. 125, no. 20, pp. 6306–6310, 2003.
- [19] L. J. Diguna, Q. Shen, J. Kobayashi, and T. Toyoda, "High efficiency of CdSe quantum-dot-sensitized TiO<sub>2</sub> inverse opal solar cells," *Applied Physics Letters*, vol. 91, no. 2, Article ID 023116, 2007.
- [20] S. Guldin, S. Hüttner, M. Kolle et al., "Dye-sensitized solar cell based on a three-dimensional photonic crystal," *Nano Letters*, vol. 10, no. 7, pp. 2303–2309, 2010.
- [21] S. Colodrero, A. Mihi, L. Hnggman et al., "Porous one-dimensional photonic crystals improve the power-conversion efficiency of dye-sensitized solar cells," *Advanced Materials*, vol. 21, no. 7, pp. 764–770, 2009.
- [22] S. Hore, P. Nitz, C. Vetter, C. Prah, M. Niggemann, and R. Kern, "Scattering spherical voids in nanocrystalline TiO<sub>2</sub> — Enhancement of efficiency in dye-sensitized solar cells," *Chemical Communications*, no. 15, pp. 2011–2013, 2005.
- [23] T. T. T. Pham, T. Bessho, N. Mathews et al., "Light scattering enhancement from sub-micrometer cavities in the photoanode for dye-sensitized solar cells," *Journal of Materials Chemistry*, vol. 22, no. 32, Article ID 16201, 2012.
- [24] P. Wang, S. M. Zakeeruddin, P. Comte, R. Charvet, R. Humphry-Baker, and M. Gratzel, "Enhance the performance of dye-sensitized solar cells by co-grafting amphiphilic sensitizer and hexadecylmalonic acid on TiO<sub>2</sub> nanocrystals," *Journal of Physical Chemistry B*, vol. 107, no. 51, pp. 14336–14341, 2003.
- [25] K. Manseki, W. Jarernboon, Y. Youhai et al., "Solid-state dye-sensitized solar cells fabricated by coupling photoelectrochemically deposited poly(3,4-ethylenedioxythiophene) (PEDOT) with silver-paint on cathode," *Chemical Communications*, vol. 47, no. 11, pp. 3120–3122, 2011.
- [26] J. X. Wang, Y. Q. Wen, H. Ge et al., "Simple Fabrication of Full Color Colloidal Crystal Films with Tough Mechanical Strength," *Macromolecular Chemistry and Physics*, vol. 207, no. 6, pp. 596–604, 2006.



**Hindawi**

Submit your manuscripts at  
<http://www.hindawi.com>

